Effect of aqueous phase cloud chemistry on tropospheric ozone

Citation

Published Version

Permanent link

Terms of Use

Share Your Story

Effect of aqueous phase cloud chemistry on tropospheric ozone

Jinyou Liang and Daniel J. Jacob

Division of Engineering and Applied Sciences and Department of Earth and Planetary Sciences, Harvard University, Cambridge, Massachusetts

Abstract. The sensitivity of tropospheric O_3 to aqueous HO_x $(OH + HO_2)$ phase chemistry in clouds is examined using photochemical model calculations of the O_3 production efficiency per unit NO_x and the chemical lifetime of O_3, combined with estimates for the residence time of air in clouds. It is found that the maximum perturbation to O_3 from cloud chemistry in the tropics and midlatitudes summer is less than 3%. This result is supported by calculations using a three-dimensional, continental-scale model for North America.

1. Introduction

Clouds modify tropospheric chemistry by scattering UV radiation, by redistributing trace constituents vertically, and also by providing relatively large volumes of liquid water for scavenging of gases and aqueous phase chemistry to take place. *Lelieveld and Crutzen* [1990] pointed out that aqueous phase chemistry in a cloud causes O_3 concentrations to decrease due to two rapid reactions involving HO_x radicals: $O_2^- + O_3(aq)$ (consuming O_3) and $HO_2(aq) + O_2^-$ (scavenging radicals). Several modeling studies have suggested that these reactions represent a significant sink for O_3 in the troposphere [*Lelieveld and Crutzen*, 1990; *Jonson and Isaksen*, 1993; *Dentener*, 1993]. However, we present here model calculations indicating that the effect on O_3 concentrations is at most a few percent, and we argue that the previous studies may have overestimated the effect.

Lelieveld and Crutzen [1990] based their analysis on photochemical model calculations of the net production minus loss rate of O_3, $(P - L)_{O_3}$, in air parcels subjected to alternating periods of clear and cloudy conditions. They found that including aqueous phase radical chemistry in their model increased the net regional O_3 loss averaged over clear and cloudy conditions by a factor of 1.3 to 2.3 under low-NO_x conditions and decreased net O_3 production by about 40% under high-NO_x conditions. On the basis of this result, they concluded that aqueous phase cloud chemistry represents a significant sink for O_3 in the troposphere. It should, however, be noted that a large relative perturbation to $(P - L)_{O_3}$ may imply only a small perturbation to O_3 concentrations, considering that P and L are of comparable magnitude in much of the troposphere [*Chameides et al.*, 1987, 1989; *Liu et al.*, 1992; *Carroll and Thompson*, 1995; *Davis et al.*, 1996; *Jacob et al.*, 1996], and that P is only weakly dependent on the O_3 concentration while L is roughly first order. In addition, the effect of cloud chemistry on O_3 cannot be decoupled from the effect on NO_x, since NO_x provides the limiting precursor for O_3 production in the troposphere. Scavenging of HO_x radicals by cloud droplets slows down the photochemical oxidation of NO_x, so that O_3 production downstream of the cloud may increase [*Dentener*, 1993]. A quantitative estimate of the effect of cloud chemistry on O_3 concentrations can still be made within the simple air parcel modeling framework of *Lelieveld and Crutzen* [1990] by choosing suitable variables as diagnostics. We present results from such an approach below.

More definite assessment of the effect of cloud chemistry on O_3 requires a chemical tracer model that can resolve the coupling between chemistry and transport. *Jonson and Isaksen* [1993] presented results from a two-dimensional (longitude-altitude) model for northern midlatitudes. They found that including clouds in their calculations (with effects on both radiation and chemistry) decreases O_3 concentrations by 10-30% relative to a simulation with only gas phase chemistry, the largest effects (20-30%) being in the middle troposphere. Their simulation assumed unusually cloudy conditions, however, with one third of the 1- to 7-km column included in cloud at any given time. In comparison, *Lelieveld et al.* [1989] estimated that clouds occupy on average 15% of the northern midlatitudes atmosphere below 4 km and occupy less at higher altitudes; we argue below that even this estimate is too high. *Jonson and Isaksen* [1993] found that including aqueous phase chemistry in their model improved the simulation of O_3 in the middle troposphere, but other O_3 models without cloud chemistry do not show a systematic problem of excessive O_3 in this part of the atmosphere [*Crutzen and Zimmerman*, 1991; *Follows and Austin*, 1992; *Müller and Brasseur*, 1995; *Roelofs and Lelieveld*, 1995].

In a pioneering study, *Dentener* [1993] included cloud chemistry in a coarse three-dimensional model with monthly averaged winds (MOGUNTIA) and compared results to a simulation including only gas phase chemistry and N_2O_5 hydrolysis in aerosols. He found that cloud chemistry causes a 5-15% decrease of O_3 concentrations in the lower troposphere and a 7% global decrease in the O_3 tropospheric inventory. We argue below that even this small effect may be an overestimate because the model assumed high liquid water abundances and high CH_3O_2 solubility.

We begin this paper (section 2) with a brief review of the aqueous phase chemistry affecting O_3 in cloud. We follow in section 3 with a conceptual model for the tropospheric O_3 budget using as variables the O_3 production efficiency (ε) and the pseudo first-order rate constant for chemical loss (k). We then present in section 4 a zero-dimensional photochemical model analysis of the sensitivity of ε and k to cloud formation, and use this analysis to estimate the perturbation to O_3 from cloud chemistry in different regions of the world. Supporting calculations using a three-dimensional model for North America are presented in section 5. Conclusions are presented in section 6.
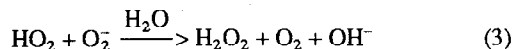
2. Cloud Chemistry and Ozone

Ozone is produced and destroyed in the troposphere by reactions involving HO_x radicals (defined as the ensemble of OH and peroxy radicals). Detailed discussions of cloud effects on HO_x chemistry have been presented by *Chameides and Davis* [1982], *Graedel and Goldberg* [1983], *Schwartz* [1984], *Jacob* [1986],
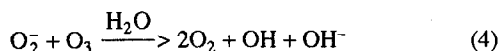
and *Lelieveld and Crutzen* [1990], among others. The HO_2 radical is scavenged efficiently by cloud droplets as a result of acid-base dissociation of $HO_2(aq)$ $(pK_a = 4.7)$:

$$HO_2(g) = HO_2(aq) \tag{1}$$

$$HO_2(aq) = H^+ + O_2^- \tag{2}$$
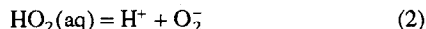
followed by electron transfer between $HO_2(aq)$ and O_2^-:

$$HO_2 + O_2^- \xrightarrow{H_2O} H_2O_2 + O_2 + OH^- \tag{3}$$

and reaction of O_2^- with $O_3(aq)$:

$$O_2^- + O_3 \xrightarrow{H_2O} 2O_2 + OH + OH^- \tag{4}$$

Cloud water pH values are typically in the range 3-5 [*Warneck*, 1988]. Model calculations by *Jacob* [1986] indicate that $HO_2(g)$ concentrations in a cloud of pH 4 are depleted by 70% relative to clear sky because of reactions (1)-(3); in a cloud of pH 5 the depletion is 85%. This depletion of $HO_2(g)$ suppresses the gas phase reaction (5), which provides the major source of O_3 in the troposphere:

$$HO_2 + NO \rightarrow OH + NO_2 \tag{5}$$

$$NO_2 + hv \xrightarrow{O_2} NO + O_3 \tag{6}$$
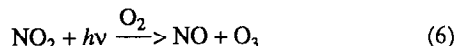
Contrary to HO_2, NO is not significantly soluble in water so that the HO_2+NO reaction does not proceed significantly in the aqueous phase. The effect of HO_2 scavenging in suppressing (5) is partly compensated in summer by an increase in the NO/NO_x ratio, as reaction with HO_2 is a significant pathway converting NO to NO_2 (reaction with O_3 dominates in winter).

Another important source of O_3 in the troposphere is (7):

$$CH_3O_2 + NO \rightarrow CH_3O + NO_2 \tag{7}$$
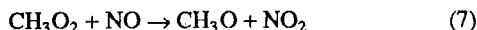
where CH_3O_2 is produced by oxidation of hydrocarbons, in particular methane. No data are available for the Henry's law constant of CH_3O_2. We expect CH_3O_2 to be far less soluble than HO_2 because of its lower polarity. By analogy, the Henry's law constant for CH_3OOH is 300 times less than that for H_2O_2 [*O'Sullivan et al.*, 1996]. Assuming the same ratio for the Henry's law constants of CH_3O_2 and HO_2, one finds that scavenging of CH_3O_2 by cloud droplets is negligible [*Jacob*, 1986]. The gas phase concentration of CH_3O_2 may actually increase in cloud due to suppression of the gas phase sink from

$$CH_3O_2 + HO_2 \rightarrow CH_3OOH + O_2 \tag{8}$$
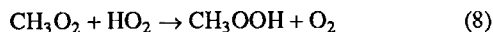
thus sustaining O_3 production in the cloud.

Scavenging of HO_2 by cloud droplets suppresses gas phase loss of O_3 by the reaction

$$HO_2 + O_3 \rightarrow OH + 2O_2 \tag{9}$$
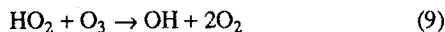
but this effect may be more than compensated by aqueous phase reaction (4) which drives the cycling of HO_x radicals in the aqueous phase (the aqueous phase reaction of HO_2 with O_3 is negligibly slow). The OH(aq) radical produced by (4) is recycled rapidly to $HO_2(aq)$ by oxidation of hydrated formaldehyde and formate [*Jacob*, 1986], leading to a HO_x-catalyzed cycle for destruction of O_3 in the aqueous phase [*Lelieveld and Crutzen*, 1990]. The efficiency of this O_3 loss cycle is limited by the aqueous phase HO_x sink from (3), which is considerably faster than the self-reaction of HO_2 in the gas phase. Reaction (3) facilitates the scavenging of HO_2 from the gas phase, on the one hand, and thus contributes to the suppression of O_3 production; on the other hand, it competes with (4) and moderates O_3 loss.
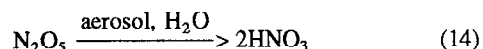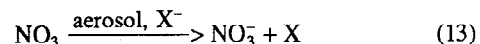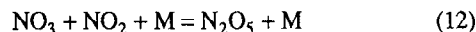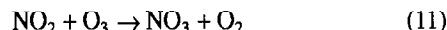
Cloud chemistry models indicate that OH(g) is depleted by 30-50% in cloud relative to clear sky conditions [*Jacob*, 1986; *Lelieveld and Crutzen*, 1990]. This depletion is due in part to

direct uptake of OH by the cloud droplets and in part to scavenging of HO_2 from the gas phase. The depletion of OH slows down NO_x oxidation in the gas phase from the reaction

$$NO_2 + OH + M \rightarrow HNO_3 + M \tag{10}$$

This reaction is further slowed by the decrease in the daytime NO_2/NO_x ratio resulting from the scavenging of HO_2 [*Dentener*, 1993]. Hence NO_x may be preserved in cloud and remain available to produce O_3 by (5) and (7) after the cloud evaporates.

An additional mechanism for NO_x loss in the troposphere is by nighttime reactions of NO_3 and N_2O_5 in aqueous aerosols:

$$NO_2 + O_3 \rightarrow NO_3 + O_2 \tag{11}$$

$$NO_3 + NO_2 + M = N_2O_5 + M \tag{12}$$

$$NO_3 \xrightarrow{aerosol, X^-} NO_3^- + X \tag{13}$$

$$N_2O_5 \xrightarrow{aerosol, H_2O} 2HNO_3 \tag{14}$$

where X^- is a suitable reductant (e.g., Cl^-). In the daytime this mechanism is suppressed by photolysis of NO_3. Cloud formation causes a large increase in the rate constants for (13)-(14), because of the increase in wet surface area [*Lelieveld and Crutzen*, 1990], but the nighttime rate of NO_x loss may not be significantly affected as it is in general limited by (11). One possibly important role of clouds is to enable the mechanism to proceed in the daytime. At the high surface areas found in cloud, (13) can compete with NO_3 photolysis, especially during winter when photolysis of NO_3 is weak.

3. A Conceptual Model for Tropospheric Ozone

Ozone production in the troposphere is limited in general by the availability of NO_x [*Chameides et al.*, 1992]. *Liu et al.* [1987] defined the O_3 production efficiency ε, as the total number of molecules of odd oxygen ($O_x = O_3 + O + NO_2 + HNO_4 + (2x)NO_3 + (3x)N_2O_5$) produced per molecule of NO_x oxidized to HNO_3. The idea is that a NO_x molecule emitted to the atmosphere undergoes a number ε of peroxy + NO conversions, producing O_x, before it is oxidized to HNO_3 which is viewed as a terminal sink. In the lower troposphere at least, HNO_3 is removed principally by deposition. Consider a region sufficiently large that NO_x is at steady state between its source E_{NO_x} and its loss L_{NO_x} (the lifetime of NO_x against oxidation is of the order of 1 day). The O_x production rate P_{O_x} can be related to E_{NO_x} by using a characteristic value of ε for the region:

$$P_{O_x} = \varepsilon E_{NO_x} \tag{15}$$

Chemical loss of O_x takes place principally by the gas phase reactions $O(^1D) + H_2O$, $HO_2 + O_3$, and $OH + O_3$, and also in cloud by the aqueous phase reaction $O_2^- + O_3(aq)$. These reactions are approximately first order in O_3, and may therefore be grouped to define a pseudo first-order loss rate constant k for O_x. Oxidation of NO_x to HNO_3 is an additional sink for O_x, but we do not include it in k because it is limited by E_{NO_x} and not directly dependent on the O_3 concentration; this subtlety is of some importance because perturbation to NO_x loss by aqueous phase chemistry should not be regarded as a real perturbation to the O_x sink (although it perturbs the O_3 production efficiency). The loss rate L_{O_x} is thus given by

$$L_{O_x} = k[O_x] + \beta E_{NO_x} \tag{16}$$

where β is the number of O_x molecules consumed in the oxidation of NO_x to HNO_3 ($\beta = 1$ for $NO_2 + OH$, $\beta = 1.5$ for N_2O_5 hydrolysis, $\beta = 2$ for $NO_3(aq) + X^-$).

Equations (15) and (16) can be combined to obtain a simple budget expression for the O_3 concentration at steady state in a

given region of the troposphere:

$$[O_3] \approx [O_x] = \frac{(\varepsilon - \beta)E_{NO_x} + F_{in}}{k + k'} \tag{17}$$

where F_{in} is the flux of O_3 into the region, and k' is a rate constant for export of O_3 out of the region including effects from both transport and deposition. In general, $\beta \ll \varepsilon$, except for high latitudes in winter. If we consider a region sufficiently large and photochemically active, so that $\varepsilon \gg \beta$, $\varepsilon E_{NO_x} \gg F_{in}$, and $k \gg k'$, then O_3 concentrations vary as ε/k. Perturbations to ε and k from cloud chemistry, as computed from a zero-dimensional air parcel model [*Lelieveld and Crutzen*, 1990], can be translated directly into a corresponding perturbation to O_3, and we follow this approach in the next section.

4. Zero-Dimensional Photochemical Model

Model Description

We compute ε and k with a zero-dimensional photochemical model for 11 air parcels representative of a range of latitudes, altitudes, and seasons [*Lelieveld and Crutzen*, 1990] (Table 1). The composition of each air parcel is defined by specified concentrations of O_3, CO, CH_4 (1.7 parts per million by volume), NO_x, and H_2O, and under cloudy conditions by a specified liquid water content (LWC) and cloud water pH. A relative humidity of 100% is assumed under both clear-sky and cloudy conditions, in order to separate the effect of aqueous phase chemistry from that of changes in humidity. The rate constant k_a for (13) and (14) under cloud-free conditions is specified following *Dentener and Crutzen* [1993]. Cloud LWCs are specified with a temperature-dependent parameterization based on *Somerville and Remer* [1984]:

$$LWC = 0.32 - 0.0060\,(T - 273)\ \text{g m}^{-3}, \tag{18a}$$

$$\text{for } 293 \geq T \geq 280\ \text{K};$$

$$LWC = 0.23 + 0.0065\,(T - 273)\ \text{g m}^{-3}, \tag{18b}$$

$$\text{for } 280 \geq T \geq 248\ \text{K};$$

$$LWC = 0.07\ \text{g m}^{-3},\ \text{for } T < 248\ \text{K} \tag{18c}$$

The cloud droplets are assumed to be monodisperse (radius = 10 μm) and of homogeneous composition, so that cloud water can be effectively modeled as a single phase defined by bulk LWC and pH. This assumption can be made with no loss of generality (we

will present calculations exploring the sensitivity to LWC and pH).

The model calculates the gas phase concentrations of $O(^1D)$, OH, HO_2, CH_3O_2, H_2O_2, CH_3OOH, CH_2O, O_2CH_2OH, HCOOH, NO, NO_2, NO_3, N_2O_5, HNO_2, and HNO_4, and when a cloud is present the aqueous phase concentrations of $O_3(aq)$, OH(aq), $HO_2(aq)$, O_2^-, $H_2O_2(aq)$, $H_2C(OH)_2(aq)$, HCOOH(aq), $HCOO^-$, $CH_3O_2(aq)$, and $CH_3OOH(aq)$. The gas phase chemical mechanism is from *DeMore et al.* [1994]. The aqueous phase chemical mechanism is from *Jacob* [1986], with updated rate constant k=7.7x10^8 M^{-1} s^{-1} for the oxidation of $H_2C(OH)_2(aq)$ by OH(aq) [*Chin and Wine*, 1994]. Gas droplet mass transfer is computed as described by *Jacob* [1986]. Ultraviolet photon intensities are calculated with the clear sky radiative transfer code of *Logan et al.* [1981]. Changes in UV radiation due to cloud formation are not considered in order to focus attention on the changes in chemistry.

For each case in Table 1, we begin by integrating to diel steady state a clear sky simulation including only gas phase chemistry and reactions of NO_3 and N_2O_5 in aerosols. Diel steady state is defined by 24-hour periodicity for the concentrations of all species being solved in the model. Once this steady state is reached, we cycle the air parcel intermittently through cloud for 7 days, using an alternating pattern of 2-hour cloudy periods followed by 12-hour cloud-free periods. This pattern was chosen to provide a cloud duration and frequency typical of the values employed by *Lelieveld and Crutzen* [1990] and also to sample cloudy conditions evenly over all times of day. Thus the 7-day simulation includes 24 hours in cloud spanning the full diel cycle of UV radiation intensities.

Values of ε and k in Cloud

Values of ε and k are retrieved from the model as

$$\varepsilon = \frac{P_{O_x}}{L_{NO_x}} \tag{19}$$

$$k = \frac{L_{O_x} - \beta\,L_{NO_x}}{[O_x]} \tag{20}$$

where the quantities on the right-hand side are 24-hour averages from the 7-day simulation, and P and L are chemical production and loss rates. Equation (20) is simply a rearrangement of (16) assuming steady state for NO_x ($E_{NO_x} = L_{NO_x}$). We calculate "with-cloud" values (ε_{wc}, k_{wc}) by sampling continuously the 7-

Table 1. Air Parcel Definitions Used in Zero-Dimensional Model

Case	Altitude km	T, K	LWC, g m^{-3}	pH	NO_x, ppt	O_3, ppb	CO, ppb	O_3 column, DU	k_a, 10^{-5}s^{-1}
1. 45°S, winter	1.5	268	0.20	5.0	10	25	70	325	5
2. 45°S, winter	3.0	260	0.15	5.0	10	25	65	325	1.5
3. 45°S, summer	1.5	285	0.25	5.0	7	15	50	300	5
4. 45°S, summer	3.0	277	0.26	5.0	7	15	50	300	1.5
5. equator	1.5	291	0.22	5.0	40	30	85	255	12
6. equator	3.0	283	0.27	5.0	30	30	75	255	2.5
7. equator	5.0	270	0.21	5.0	20	30	70	255	1
8. 45°N, winter	1.5	268	0.20	4.5	780	30	130	350	27
9. 45°N, winter	3.0	260	0.15	4.5	400	30	115	350	12
10. 45°N, summer	1.5	285	0.25	4.5	135	40	90	315	27
11. 45°N, summer	3.0	277	0.26	4.5	100	40	85	315	12

The air parcel compositions are from *Lelieveld and Crutzen* [1990]. The cloud liquid water contents (LWC) are from equation (18). The rate constants k_a for conversion of NO_3 and N_2O_5 to HNO_3 in aerosols under noncloudy conditions are from *Dentener and Crutzen* [1993]. Abbreviation ppt, parts per trillion volume; ppb, parts per billion volume; DU, Dobson units (1 DU = 2.687 x10^{16} molecules cm^{-2}).
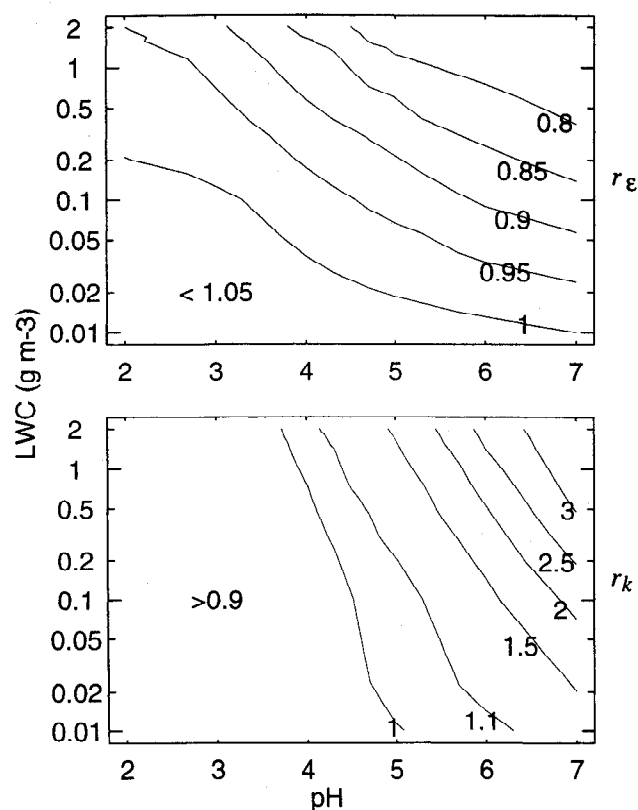
Figure 1. Relative effect of aqueous phase HO_x chemistry on the in-cloud values of (top) the local O_3 production efficiency ε per unit NO_x consumed and (bottom) the pseudo first-order rate constant k for O_x chemical loss. The contours show the ratios $r_\varepsilon = \varepsilon_{cl}/\varepsilon_{nc}$ and $r_k = k_{cl}/k_{nc}$ of ε and k calculated in a cloudy air parcel with (cl) versus without (nc) consideration of aqueous phase chemistry. Results are for case 5 of Table 1 (equator, 1.5-km altitude) and are presented as a function of cloud water pH and liquid water content (LWC).

day simulation with alternating cloudy and clear sky periods, and calculate "cloudy" values (ε_{cl}, k_{cl}) by sampling cloudy periods only from that simulation (i.e., combining the twelve 2-hour cloudy periods from the 7-day simulation to yield a 24-hour in-cloud average). To provide a reference against which to assess the effect of cloud chemistry, we also calculate "no-cloud" values (ε_{nc}, k_{nc}) by conducting a 7-day simulation including gas and

aerosol chemistry but no aqueous phase HO_x radical chemistry in cloud. This "no-cloud" simulation still accounts for the increased loss of NO_3 and N_2O_5 in intermittent clouds due to the surface-limited reactions (13) and (14); assessment of a cloud effect associated with these reactions would be ambiguous as it depends on the aerosol surface area assumed to represent cloud-free conditions. The rate constants k_a for (13)-(14) given in Table 1 are based on average relative humidity conditions [*Dentener and Crutzen*, 1993] and would underestimate values for a pre-cloud atmosphere at 100% relative humidity.

Figure 1 shows the sensitivities of ε and k in cloud to aqueous phase radical chemistry, as expressed by the ratios of "cloudy" to "no-cloud" values,

$$r_\varepsilon = \frac{\varepsilon_{cl}}{\varepsilon_{nc}} \tag{21}$$

$$r_k = \frac{k_{cl}}{k_{nc}} \tag{22}$$

for the air parcel of case 5 (equator, 1.5-km altitude) as a function of cloud LWC and pH. We see from Figure 1 that aqueous phase chemistry has less than 20% effects on in-cloud values of ε and k over the usual range of LWC (0.1-0.5 g m^{-3}) and pH (3-5). These weak effects reflect in part the compensating factors discussed in section 2. Another factor moderating the effect on k is that most of the gas phase loss of O_x is by the reaction $O(^1D)+H_2O$, which is unaffected by cloud chemistry. For pH values above 5 (pH > $pK_a(HO_2/O_2^-)$) the effect of cloud chemistry on k increases rapidly with pH because of (2) and (4) and also because of the suppression of (3) which competes with (4). Results in Figure 1 indicate that k may increase by as much as 50% relative to clear sky inside a dense cloud with pH 5, such as in the upward regions of convective storms [*Barth et al.*, 1992]. However, air spends little time in such dense clouds, which occupy little atmospheric volume.

Table 2 shows the effects of cloud chemistry on ε and k for different regions and seasons, as illustrated by the 11 cases of Table 1. Aqueous phase chemistry decreases in-cloud values of ε by 0-40% in the tropics and midlatitudes summer, and by 50-70% in midlatitudes winter; k increases by 0-30% in the former cases and by 70-90% in the latter cases. In winter the compensating factor on ε from reduced photochemical loss of NO_x is relatively small because nighttime reactions of NO_3 and N_2O_5 in aerosols provide the principal sink for NO_x [*Dentener and Crutzen*, 1993].

Table 2. Effect of Cloud Chemistry on O_3 concentrations

Case	$\dfrac{P^{cl}_{O_x}}{P^{nc}_{O_x}}$	$\dfrac{L^{cl}_{NO_x}}{L^{nc}_{NO_x}}$	ε_{nc}	ε_{cl}	k_{nc},	k_{cl},	f,	$\max(-\dfrac{\Delta[O_3]}{[O_3]})$,
			mol/mol	mol/mol	d^{-1}	d^{-1}	%	%
1	0.33	0.94	13	4.5	0.0099	0.017	11	14
2	0.25	0.95	12	3.3	0.0069	0.012	11	16
3	0.83	0.80	64	66	0.15	0.18	7.4	1.0
4	0.71	0.73	82	80	0.11	0.14	9.0	2.3
5	0.79	0.88	25	22	0.33	0.37	6.0	1.1
6	0.73	0.82	29	26	0.24	0.28	5.6	1.4
7	0.60	0.75	44	35	0.12	0.15	3.1	1.3
8	0.39	0.86	1.8	0.83	0.0062	0.012	11	28
9	0.22	0.77	4.5	1.3	0.0068	0.013	11	17
10	0.47	0.70	17	12	0.17	0.18	9.9	2.5
11	0.38	0.63	24	14	0.13	0.13	11	3.2

Results are shown for the 11 air parcel cases of Table 1. The indices "cl" and "nc" refer to 24-hour average quantities computed in cloudy air parcels, with and without consideration of aqueous phase radical chemistry, respectively. $\max(-\Delta[O_3]/[O_3])$ is the theoretical maximum relative decrease of the regional O_3 concentration due to cloud chemistry, as calculated from (28), assuming that clouds occupy a volume fraction of f of the regional atmosphere.

During winter, uptake of NO_3 and N_2O_5 by cloud droplets can compete with NO_3 photolysis during daytime hours, further reducing the importance of OH as a NO_x oxidant. Despite the relatively high perturbations to ε and k, the effect of cloud chemistry on O_3 concentrations in winter should be weak considering that the chemical lifetime of O_3 is several months, even in cloud (Table 2).

Ozone Budget Perturbation

The above discussion focused on the perturbation to in-cloud values of ε and k from aqueous phase chemistry. However, an air parcel is cloudy only a fraction of the time. The perturbation to O_3 concentrations from intermittent cloud chemistry in the 11 cases of Table 1 can be estimated from (17) by using "with-cloud" versus "no-cloud" values of $(\varepsilon - \beta)$ (hereinafter denoted as ε for simplicity of notation) and k. The magnitude of the perturbation depends on the fraction f of time that the air parcel is cloudy. We find in our model that a simple linear relationship can be used to relate the average "with-cloud" values $(\varepsilon_{wc}, k_{wc})$ to the previously discussed "cloudy" values $(\varepsilon_{cl}, k_{cl})$ and "no-cloud" values $(\varepsilon_{nc}, k_{nc})$:

$$\varepsilon_{wc} \approx \frac{(1-f)P^{nc}_{O_x} + f P^{cl}_{O_x}}{(1-f)L^{nc}_{NO_x} + f L^{cl}_{NO_x}} = w\,\varepsilon_{nc} + (1-w)\,\varepsilon_{cl} \quad (23)$$

$$k_{wc} \approx (1-f)k_{nc} + f k_{cl} \quad (24)$$

where

$$w = \frac{1-f}{1-f+f\,r_L} \quad (25)$$

$$r_L = \frac{L^{cl}_{NO_x}}{L^{nc}_{NO_x}} \quad (26)$$

and the indices "cl" and "nc" refer to the "cloudy" and "no-cloud" values as previously defined. Replacing into our O_3 budget equation (17), we obtain the following expression for the relative decrease of O_3 in the air parcel due to cloud chemistry:

$$\frac{[O_3]^{nc} - [O_3]^{wc}}{[O_3]^{nc}} \equiv -\frac{\Delta[O_3]}{[O_3]} = 1 - \frac{w + (1-w)\,r_\varepsilon + \dfrac{F_{in}}{\varepsilon_{nc}E_{NO_x}}}{1 + \dfrac{F_{in}}{\varepsilon_{nc}E_{NO_x}}}$$

$$\cdot \frac{1 + \dfrac{k'}{k_{nc}}}{1 - f + f\,r_k + \dfrac{k'}{k_{nc}}} \quad (27)$$

For all our cases except case 3, $r_\varepsilon < 1$ and $r_k > 1$, so that the O_3 perturbation is largest when the regional O_3 budget is controlled solely by chemical production and loss ($\varepsilon E_{NO_x} \gg F_{in}$, $k \gg k'$). From (27) we obtain the following upper limit for the relative decrease of O_3 concentrations due to cloud chemistry:

$$\max(-\frac{\Delta[O_3]}{[O_3]}) = 1 - \frac{w + (1-w)\,r_\varepsilon}{1-f+f\,r_k} \quad (28a)$$

In case 3, $r_\varepsilon > 1$ and $r_k > 1$, so that the O_3 perturbation is largest when the regional O_3 budget is controlled solely by transport and chemical loss ($F_{in} \gg \varepsilon E_{NO_x}$, $k \gg k'$). The upper limit for the perturbation in this case is

$$\max(-\frac{\Delta[O_3]}{[O_3]}) = 1 - \frac{1}{1-f+f\,r_k} \quad (28b)$$

We estimate values of f for cases 1-11 in Table 1 by constraining the resulting time-averaged liquid water in the 0- to 5-km column to match global satellite observations of liquid water columns reported by Greenwald et al. [1993] for that latitude (Figure 2). This approach yields values of f ranging from 3 to 11% depending on the case, with most around 10%. The resulting maximum decrease of O_3 concentrations from cloud chemistry is only 1-3% in the tropics and in midlatitudes summer (Table 2). Larger values for the maximum decrease are found for midlatitudes winter; however, transport terms dominate the O_3 budget during that time of year [Levy et al., 1985], so that the actual perturbation to O_3 is certainly much less than the theoretical maximum.

The perturbations to O_3 from cloud chemistry reported here are much smaller than in the previous modeling studies of Lelieveld and Crutzen [1990], Jonson and Isaksen [1993], and Dentener [1993]. The assumption of large liquid water abundances in these studies is an important factor in the discrepancy. We compare in Figure 2 the liquid water column climatologies assumed by Lelieveld and Crutzen [1990] and Dentener [1993] to the satellite observations of Greenwald et al. [1993] and Njoku and Swanson [1983]; the observations are consistently lower. As pointed out in the Introduction, the model study of Jonson and Isaksen [1993] assumed even higher liquid water columns.
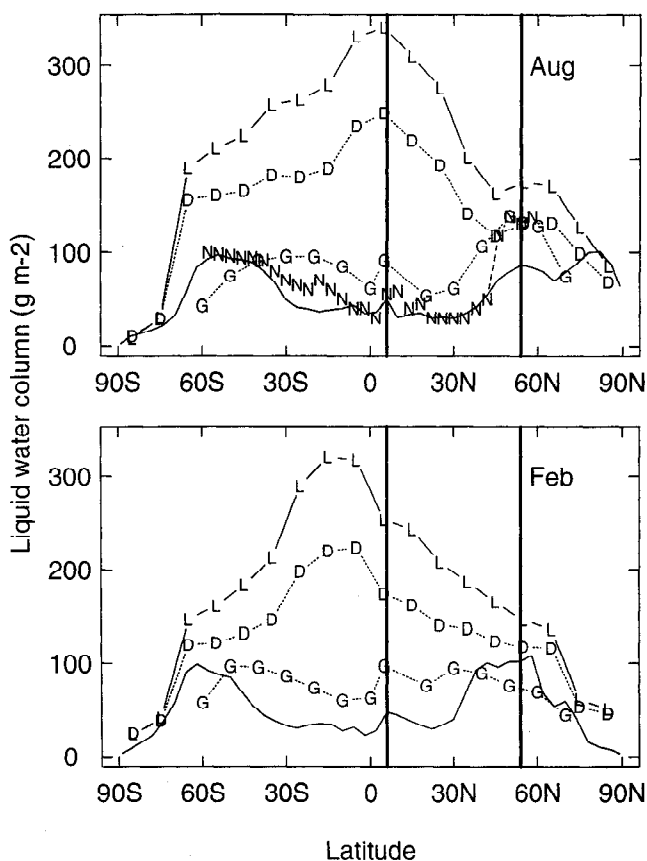
Figure 2. Zonally averaged atmospheric liquid water columns in (top) August and (bottom) February as a function of latitude. Satellite observations (ocean only) from Greenwald et al. [1993] and Njoku and Swanson [1983] are shown as "G" and "N" symbols, respectively. The seasonal climatologies used in the models of Lelieveld and Crutzen [1990] (as given by Lelieveld et al. [1989]) and Dentener [1993] are shown as "L" and "D" symbols, respectively. The solid line shows the GISS GCM values calculated as described in section 5. The two thick vertical lines bracket the latitudes analyzed in our three-dimensional model.

Another factor responsible for the higher sensitivities of O_3 to cloud chemistry found in previous modeling studies is that these studies assumed a high Henry's law constant (K) for CH_3O_2, equal to that of HO_2 ($K_{CH_3O_2} = K_{HO_2} = 2000$ M atm^{-1} at $T=298$ K). As pointed out in section 2, the Henry's law constant for CH_3O_2 is likely less than that for HO_2. We have used $K_{CH_3O_2} = 5.9$ M atm^{-1} (at $T=298$ K) in our standard model by assuming that the ratio of the Henry's law constants for CH_3O_2 and HO_2 is equal to that for CH_3OOH and H_2O_2 [*Jacob*, 1986]. We conducted a sensitivity test for the cases in Table 1 using $K_{CH_3O_2} = 2000$ M atm^{-1} ($T=298$ K) and $CH_3O_2(aq)$ chemistry in cloud based on similarity with $HO_2(aq)$ [*Jacob*, 1986]. The production of O_3 in cloud is more strongly suppressed than in our standard model, with $r_\varepsilon = 0.47$-0.73 in the tropics and midlatitudes summer. The perturbation to k is unaffected. The maximum decrease of O_3 concentrations from cloud chemistry is 2-5% in the tropics and midlatitudes summer, about twice the values computed in our standard model.

The Henry's law constant for HO_2 has an uncertainty of about a factor of 2 [*Schwartz*, 1984]. To evaluate the effect of this uncertainty, we performed another sensitivity test for the cases in Table 1 by doubling the Henry's law constant of HO_2. We find that the perturbation to O_3 from cloud chemistry is not sensibly increased over that in our standard model, an expected result since the solubility of HO_2 in our standard model is already sufficiently high for efficient scavenging of HO_2 from the gas phase.

5. Three-Dimensional Model for North America

Our conceptual model analysis of sections 3-4 oversimplifies the chemistry of tropospheric O_3 by treating the atmosphere as regionally homogeneous and neglecting the coupling between chemistry and transport. As a test of our conclusions from this conceptual model, we examine here the sensitivity of O_3 to cloud chemistry with a three-dimensional continental-scale model for North America originally described by *Jacob et al.* [1993]. The version of the model used here features a number of improvements, particularly in the formulation and integration of the chemical mechanism.

Model Description

The model simulates O_3-NO_x-CO-hydrocarbon chemistry over a domain extending horizontally from the mid-Pacific (162.5°W) to the mid-Atlantic (27.5°W), from the tropics (4°N) to the subarctic (56°N), and vertically from the surface to the stratosphere. The grid resolution is 4°x5° in the horizontal, with nine layers in the vertical and a time step of 4 hours. The four lowest layers are centered at 980, 915, 810, and 655 hPa for a grid square at sea level. A subgrid nested scheme accounts for chemical nonlinearities in urban and industrial plumes [*Sillman et al.*, 1990]. Meteorological input including cloud optical depths in individual grid boxes is provided by an archive of 4-hour resolution data from a general circulation model (GCM) developed at the Goddard Institute of Space Studies (GISS) [*Hansen et al.*, 1983]. Boundary conditions for O_3 and other tracers at the edges of the model domain are specified by observed concentrations over the western Pacific from the Pacific Exploratory Mission PEM-West(A) [*Davis et al.*, 1996]. These observations are interpolated on the latitude-altitude grid of the model.

Twenty-one tracers are transported in the model including O_3, CO, NO_x, four nonmethane hydrocarbons (propane, butane, propene, isoprene), and their oxidation products. The gas phase chemical mechanism is based on recent compilations [*DeMore et al.*, 1994; *Atkinson*, 1994; *Atkinson et al.*, 1993]. Photolysis rates are calculated with a radiative transfer code [*Logan et al.*, 1981],

including cloud albedos at 800, 500, and 200 hPa inferred from GCM cloud optical depths. Conversion of NO_3 and N_2O_5 in aerosols is treated by assuming a reaction probability of 0.1 at the aerosol surface [*Dentener and Crutzen*, 1993]. The aerosol surface area is estimated from a three-dimensional simulation of sulfate employing the GCM meteorological environment [*Chin et al.*, 1996] and assuming the aerosol to be $NH_4HSO_4 \cdot nH_2O$ (where n is defined by the local relative humidity). The aqueous phase cloud chemistry mechanism is the same as in section 4. A cloud water pH of 4.5 is assumed. Over a 4-hour model time step a grid box is assumed to be 100% cloudy for a fraction f of the time corresponding to the cloud volume fraction of the grid box, and 100% clear for a fraction ($1 - f$) of the time. The calculation of f is described below.

Anthropogenic emissions of NO_x, hydrocarbons, and CO in North America are from a high-resolution inventory for 1985 produced by the U.S. *Environmental Protection Agency (EPA)* [1989] and are scaled to national estimates of emissions for 1990 [*EPA*, 1993]. Biogenic emission of isoprene is calculated using the inventory of *Guenther et al.* [1995]. Dry deposition fluxes of species are computed following *Wesely* [1989], and scavenging of HNO_3 and H_2O_2 by precipitation is computed following *Balkanski et al.* [1993].

Integration of the chemical mechanism including emission and dry deposition is done with a fast Gear solver [*Jacobson and Turco*, 1994]; an implicit finite difference method [*Wofsy*, 1978] is employed in cases involving aqueous phase chemistry where the Gear solver requires excessively small time steps for integration. Because of the short lifetime of OH(aq), aqueous phase chemistry greatly enhances the stiffness of the model chemical system.

The cloud volume fraction f of a grid box for a given time step is calculated from the liquid water column Λ (g m^{-2}) in the grid box, the vertical thickness ΔZ (meters) of the grid box, and the LWC (g m^{-3}) from (18):

$$f = \frac{\Lambda}{\Delta Z \, LWC} \qquad (29)$$

We retrieve Λ from the cloud optical depth τ in the grid box as follows [*Lin and Rossow*, 1994]:

$$\Lambda = \frac{4\tau r_e \rho_w}{3Q_{ext}} \qquad (30)$$

where $\rho_w = 1$ g cm^{-3} is the density of liquid water, $Q_{ext} \approx 2$ is the extinction coefficient, and r_e is an effective cloud droplet radius. For liquid water clouds $r_e = 10$ μm is appropriate [*Lin and Rossow*, 1994].

We compare in Figure 2 the resulting zonal mean liquid water columns computed from the GISS GCM to the satellite observations of *Njoku and Swanson* [1983] and *Greenwald et al.* [1993]. The GCM values in August agree well with *Njoku and Swanson* [1983] but both are smaller than *Greenwald et al.*'s [1993] by up to 50%. The GCM values for February are also smaller by up to 50% than those of *Greenwald et al.* [1993]. Although the discrepancy is within the uncertainty of the measurements, estimated at 50 g m^{-2} [*Greenwald et al.*, 1993], it appears that the GCM may underestimate cloud water abundances. Sensitivity simulations with increased cloud water abundances will be presented below.

Results

We conducted simulations for two 2-month periods, June-July and January-February, starting from the boundary conditions as initial conditions. The first month was used for initialization (1 month is sufficient to ventilate the model domain). We present results for July and February. Figure 3 shows the monthly mean concentrations of O_3 and NO_x simulated for these 2 months. We focus our attention on the U.S. boundary layer, defined as the
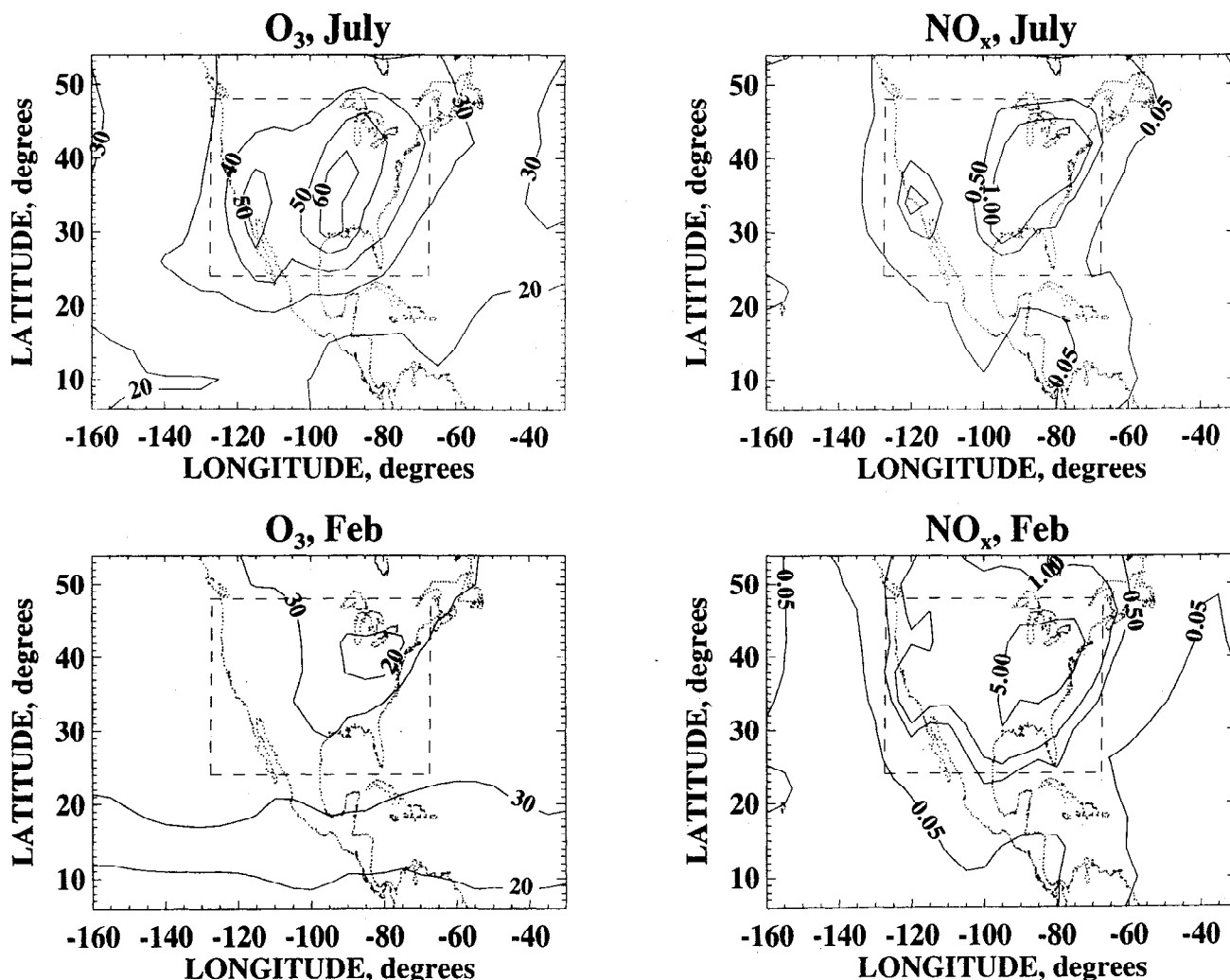
Figure 3. Monthly mean concentrations of O_3 and NO_x (ppb) calculated by the three-dimensional model in the mixed layer (~200 m above the surface) in July and February. The dashed line defines the perimeter of the U.S. boundary layer used in O_3 budget calculations.

region extending horizontally from 24°N to 48°N and from 127.5°W to 67.5°W (Figure 3), and vertically to the top of the third model layer (about 740 hPa, or 2.6 km altitude). This region is far from the boundaries of the model domain and receives high NO_x emissions, so that NO_x concentrations are not significantly affected by advection of boundary conditions.

Table 3 shows model results for the U.S. boundary layer obtained for (1) a standard "gas-aerosol-cloud" simulation using the model as described above; (2) a "gas-aerosol" simulation ignoring aqueous phase chemistry in cloud; (3) a "gas-only" simulation ignoring also the reactions of NO_3 and N_2O_5 in aerosols; and (4) a "gas-cloud" simulation ignoring the reactions of NO_3 and N_2O_5 in aerosols but including aqueous phase chemistry in cloud. The "gas-aerosol-cloud" simulation was conducted for the standard specifications of cloud abundances and pH described above and also for sensitivity cases with tripled cloud volume and pH increased to 7. Changes in O_3 concentrations between the different simulations are minuscule (Table 3), in part due to the advection of O_3 from the model boundaries. We focus our comparisons on the regional O_3 production rate and the lifetime of O_3 against chemical loss ($[O_3]/L_{O_x}$), which are not sensitive to the boundary conditions.

The results in Table 3 show that including cloud chemistry in the model ("gas-aerosol" versus "gas-aerosol-cloud") decreases regional O_3 production by less than 1% in summer and by 6% in

winter; the lifetime of O_3 against chemical loss decreases by less than 1% in summer and by only 2% in winter. Including cloud chemistry in the model without reactions in aerosols ("gas-cloud" versus "gas-only"), or without nonmethane hydrocarbons (not shown), has similarly small effects. Tripling the cloud volumes ($f \times 3$) in the summer case roughly triples the O_3 perturbation; the effect is still small. As an extreme case, we conducted a sensitivity simulation with tripled cloud volume and a cloud water pH of 7 ("$f \times 3$, $pH=7$") in summer. Only then does the effect of cloud chemistry on O_3 become significant, as shown in Table 3 (21% decrease in the chemical lifetime of O_3 relative to the gas-aerosol simulation).

6. Conclusions

We examined the sensitivity of tropospheric O_3 to aqueous phase HO_x chemistry in clouds by conducting zero-dimensional model calculations of the O_3 production efficiency per unit NO_x consumed (ε) and of the lifetime of O_3 against chemical loss ($1/k$) with and without aqueous phase chemistry. Results for the tropics and for midlatitudes summer indicate that aqueous phase chemistry causes in-cloud values of ε to decrease by 0-40% and the in-cloud chemical lifetime of O_3 to decrease by 0-25%. Cloud formation suppresses O_3 production (mainly by scavenging of HO_2) but also slows down the loss of NO_x (due to scavenging of

LIANG AND JACOB: AQUEOUS PHASE CLOUD CHEMISTRY

Table 3. Three-Dimensional Model Budgets of O_3 and NO_x in the U.S. Boundary Layer

Simulation	Production of O_x, ppb d^{-1}	Loss of O_x, ppb d^{-1}	O_3, ppb	NO_x, ppb
July				
Gas-only	12.8	7.34	49.1	0.236
Gas-cloud	12.7	7.34	48.8	0.237
Gas-aerosol	12.2	7.18	48.1	0.217
Gas-aerosol-cloud				
Standard ($f = 0.04$, pH=4.5)	12.1	7.18	47.8	0.218
$f \times 3$, pH=4.5	11.9	7.19	46.9	0.217
$f \times 3$, pH=7	12.0	8.17	43.3	0.228
February				
Gas-only	2.61	1.99	38.3	0.866
Gas-cloud	2.47	2.00	37.9	0.893
Gas-aerosol	2.48	2.02	37.9	0.787
Gas-acrosol-cloud				
Standard ($f = 0.09$, pH=4.5)	2.33	2.03	37.5	0.813

All quantities are monthly averages for the U.S. boundary layer calculated with the continental-scale three-dimensional model. The "gas only" simulation includes no aerosol or cloud reactions. The "gas-cloud" simulation includes aqueous phase cloud chemistry but no aerosol reactions. The "gas-aerosol" simulation includes reactions of N_2O_5 and NO_3 in aerosols but no cloud chemistry. The "gas-acrosol-cloud" simulation includes both cloud chemistry and reactions of N_2O_5 and NO_3 in aerosols; results of sensitivity calculations with increased cloud water pH and increased cloud volume fraction (f) are also shown.

OH), moderating the effect on the O_3 production efficiency. Based on typical frequencies of air processing by clouds, we estimate that the maximum perturbation to O_3 concentrations from cloud chemistry in the tropics and midlatitudes summer is 1-3%. Calculations with a three-dimensional model for North America support this result.

Our estimates of the perturbation to O_3 from aqueous phase cloud chemistry are considerably lower than reported in previous model studies [*Lelieveld and Crutzen*, 1990; *Dentener*, 1993; *Jonson and Isaksen*, 1993]. The difference reflects in part our use of lower cloud liquid water abundances constrained with recent observations. Another contributing factor is that our study assumes a much smaller, and we argue more realistic, solubility of CH_3O_2.

We conclude that based on current chemical knowledge there is little justification for including aqueous phase HO_x chemistry in regional and global models of tropospheric O_3, particularly in view of the computational penalty associated with the increased stiffness of the chemical system. Hydrolysis of NO_3 and N_2O_5 in aerosols and clouds is far more important for modifying O_3 concentrations and can be included in models as a surface-limited process without explicit consideration of aqueous phase chemical reactions [*Dentener*, 1993; *Dentener and Crutzen*, 1993].

Our conclusion needs to be qualified in two ways. First, significant perturbation to O_3 concentrations from aqueous phase cloud chemistry might be found in regions such as stratus-capped marine boundary layers in the tropics where clouds occupy a large volume fraction and where UV radiation is particularly intense near cloud top. Second, important aqueous phase radical sources might be missing from current cloud chemistry mechanisms, for example, photochemical reactions involving trace metals or dissolved organic compounds [*Graedel et al.*, 1986; *Faust et al.*, 1993; *Zuo and Hoigne*, 1993; *Siefert et al.*, 1996]. Not enough is known presently about these missing reactions to allow quantitative inclusion in models. As more information becomes available, an assessment of their effects on tropospheric O_3 can be made using the simple zero-dimensional modeling approach described in this paper.

References

Atkinson, R.A., Gas phase tropospheric chemistry of organic compounds, *J. Phys. Chem. Ref. Data*, 22, 1-261, 1994.

Atkinson, R.A., D.L. Baulch, R.A. Cox, R.F. Hampson Jr., J.A. Kerr, and J. Troe, Evaluated kinetic and photochemical data for atmospheric chemistry, supplement V, IUPAC subcommittee on gas kinetic data evaluation for atmospheric chemistry, *J. Phys. Chem. Ref. Data*, 21, 1125-1568, 1993.

Balkanski, Y.J., D.J. Jacob, G.M. Gardner, W.M. Graustein, and K.K. Turekian, Transport and residence times of continental aerosols inferred from a global three-dimensional simulation of ^{210}Pb, *J. Geophys. Res.*, 98, 20,573-20,586, 1993.

Barth, M.C., D.A. Hegg, and P.V. Hobbs, Numerical modeling of cloud and precipitation chemistry associated with two rainbands and some comparisons with observations, *J. Geophys. Res.*, 97, 5825-5845, 1992.

Carroll, M.A. and A.M. Thompson, NO_x in the non-urban troposphere, in *Advances in Physical Chemistry*, edited by J. Barker, World Sci., River Edge, N. J., 1995.

Chameides, W.L., and D.D. Davis, The free radical chemistry of cloud droplets and its impact upon the composition of rain, *J. Geophys. Res.*, 87, 4863-4877, 1982.

Chameides, W.L., D.D. Davis, M.O. Rodgers, J. Bradshaw, S. Sandholm, G. Sachse, G. Hill, G. Gregory, and R. Rasmussen, Net ozone photochemical production over the eastern and central North Pacific as inferred from GTE/CITE 1 observations during fall 1983, *J. Geophys. Res.*, 92, 2131-2152, 1987.

Chameides, W.L., D.D. Davis, G.L. Gregory, G. Sachse, and A.L. Torres, Ozone precursors and ozone photochemistry over eastern North Pacific during the spring of 1984 based on the NASA GTE/CITE 1 airborne observations, *J. Geophys. Res.*, 94, 9799-9808, 1989.

Chameides, W.L., et al., Ozone precursor relationships in the ambient atmosphere, *J. Geophys. Res.*, 97, 6037-6055, 1992.

Chin, M., and P.H. Wine, A temperature dependent competitive kinetic study of the aqueous phase reactions of OH radicals with formate, formic acid, acetate, acetic acid, and hydrated formaldehyde, in *Environmental Aspects of Surface and Aquatic Photochemistry*, edited by G. Helz, R. Zepp, and D. Crosby, pp. 85-98, A. F. Lewis, New York, 1994.

Chin, M., D.J. Jacob, G.M. Gardner, M.S. Foreman-Fowler, P.A. Spiro, and D.L. Savoie, A global three-dimensional model of tropospheric sulfate, *J. Geophys. Res., 101*, 18,667-18,690, 1996.

Crutzen, P.J., and P.H. Zimmermann, The changing photochemistry of the troposphere, *Tellus, 43AB*, 136-151, 1991.

Davis, D.D., et al., Assessment of ozone photochemistry in the western North Pacific as inferred from PEM-West A observations during the fall 1991, *J. Geophys. Res., 101*, 2111-2134, 1996.

DeMore, W.B., S.P. Sander, D.M. Golden, R.F. Hampson, M.J. Kurylo, C.J. Howard, A.R. Ravishankara, C.E. Kolb, and M.J. Molina, Chemical kinetics and photochemical data for use in stratospheric modeling, Evaluation No. 9, *JPL Publ., 94-1*, Jet Propul. Lab., Pasadena, Calif., 1994.

Dentener, F.J., Heterogeneous chemistry in the troposphere, Ph.D. thesis, Univ. of Utrecht, Utrecht, Netherlands, 1993.

Dentener, F.J., and P.J. Crutzen, Reaction of N_2O_5 on tropospheric aerosols: Impact on the global distribution of NO_x, O_3, and OH, *J. Geophys. Res., 98*, 7149-7163, 1993.

Faust, B.C., C. Anastasio, J.M. Allen, and T. Arakaki, Aqueous phase photochemical formation of peroxides in authentic cloud and fog waters, *Science, 260*, 73-75, 1993.

Follows, M.J., and J.F. Austin, A zonal average model of the stratospheric contributions to the tropospheric ozone budget, *J. Geophys. Res., 97*, 18,047-18,060, 1992.

Graedel, T.E., and K.I. Goldberg, Kinetic studies of raindrop chemistry, 1, Inorganic and organic processes, *J. Geophys. Res., 88*, 10,865-10,882, 1983.

Graedel, T.E., M.L. Mandich, and C.J. Weschler, Kinetic model studies of atmospheric droplet chemistry, 2, Homogeneous transition metal chemistry in raindrops, *J. Geophys. Res., 91*, 5205-5221, 1986.

Greenwald, T.J., G.L. Stephens, T.H. Vonder Haar, and D.L. Jackson, A physical retrieval of cloud liquid water over the global oceans using special sensor microwave/imager (SSM/I) observations, *J. Geophys. Res., 98*, 18,471-18,488, 1993.

Guenther, A., et al., A global model of natural volatile organic compound emissions, *J. Geophys. Res., 100*, 8873-8892, 1995.

Hansen, J., G. Russell, D. Rind, P. Stone, A. Lacis, S. Lebedeff, R. Ruedy, and L. Travis, Efficient three-dimensional global models for climate studies: Models I and II, *Mon. Weather. Rev., 111*, 609-662, 1983.

Jacob, D.J., Chemistry of OH in remote clouds and its role in the production of formic acid and peroxymonosulfate, *J. Geophys. Res., 91*, 9807-9826, 1986.

Jacob, D.J., et al., Simulation of summertime ozone over North America, *J. Geophys. Res., 98*, 14,797-14,816, 1993.

Jacob, D.J., et al., The origin of ozone and NO_x in the tropical troposphere: A photochemical analysis of aircraft observations over the South Atlantic basin, *J. Geophys. Res., 101fR*, 24,235-24,250, 1996.

Jacobson, M.Z., and R.P. Turco, SMVGEAR: A sparse-matrix, vectorized Gear code for atmospheric models, *Atmos. Environ., 28(A)*, 273-284, 1994.

Jonson, J.E., and I.S.A. Isaksen, Tropospheric ozone chemistry: The impact of cloud chemistry, *J. Atmos. Chem., 16*, 99-122, 1993.

Lelieveld, J., and P.J. Crutzen, Influence of cloud photochemical processes on tropospheric ozone, *Nature, 343*, 227-233, 1990.

Lelieveld, J., P.J. Crutzen, and H. Rodhe, Zonal average cloud characteristics for global atmospheric chemistry modelling, *Rep. CM-76*, Dep. of Meteorol., Univ. of Stockholm, Stockholm, 1989.

Levy, H., II, J.D. Mahlman, W.J. Moxim, and S.C. Liu, Tropospheric ozone: The role of transport, *J. Geophys. Res., 90*, 3753-3772, 1985.

Lin, B., and W.B. Rossow, Observations of cloud liquid water path over oceans: Optical and microwave remote sensing methods, *J. Geophys. Res., 99*, 20,907-20,927, 1994.

Liu, S.C., M. Trainer, F.C. Fehsenfeld, D.D. Parrish, E.J. Williams, D.W. Fahey, G. Hubler, and P.C. Murphy, Ozone production in the rural troposphere and the implications for regional and global ozone distributions, *J. Geophys. Res., 92*, 4191-4207, 1987.

Liu, S.C., et al., A study of the photochemistry and ozone budget during the Mauna Loa Observatory photochemistry experiment, *J. Geophys. Res., 97*, 10,463-10,471, 1992.

Logan, J.A., M.J. Prather, S.C. Wofsy, and M.B. McElroy, Tropospheric chemistry: A global perspective, *J. Geophys. Res., 86*, 7210-7254, 1981.

Müller, J.F. and G. Brasseur, Images: A three-dimensional chemical-transport model of the global troposphere, *J. Geophys. Res., 100*, 16,445-16,490, 1995.

Njoku, E.G., and L. Swanson, Global measurements of sea surface temperature, wind speed and atmospheric water content from satellite microwave radiometry, *Mon. Weather Rev., 111*, 1977-1987, 1983.

O'Sullivan, D.W., M. Lee, B.C. Noone, and B.G. Heikes, Henry's Law constant determinations for hydrogen peroxide, methylhydroperoxide, hydroxymethylhydroperoxide, ethylhydroperoxide and peroxyacetic acid, *J. Phys. Chem., 100*, 3241-3247, 1996.

Roelofs, G.J., and J. Lelieveld, Distribution and budget of O_3 in the troposphere calculated with a chemistry general circulation model, *J. Geophys. Res., 100*, 20,983-20,998, 1995.

Schwartz, S.E., Gas and aqueous phase chemistry of HO_2 in liquid water clouds, *J. Geophys. Res., 89*, 11,589-11,598, 1984.

Siefert, R.L., S.M. Webb, and M.R. Hoffmann, Determination of photochemically available iron in ambient aerosols, *J. Geophys. Res., 101*, 14,441-14,449, 1996.

Sillman, S., J.A. Logan, and S.C. Wofsy, A regional scale model for ozone in the United States with subgrid representation of urban and power plant plumes, *J. Geophys. Res., 95*, 5731-5748, 1990.

Somerville, R.C.J., and L.A. Remer, Cloud optical thickness feedbacks in the CO_2 climate problem, *J. Geophys. Res., 89*, 9668-9672, 1984.

U. S. Environmental Protection Agency (EPA), The 1985 NAPAP emission inventory (version 2): Development of the annual data and modeler's tapes, *Rep. EPA-600/7-89-012a*, Research Triangle Park, N. C., 1989.

U. S. Environmental Protection Agency (EPA), National air pollutant emissions estimates, 1900-1992, *Rep. EPA-454/R-93-032*, Research Triangle Park, N. C., 1993.

Warneck, P., *Chemistry of the Natural Atmosphere*, Academic, San Diego, Calif., 1988.

Wesely, M.L., Parameterization of surface resistance to gaseous dry deposition in regional-scale numerical models, *Atmos. Environ., 23*, 1292-1304, 1989.

Wofsy, S.C., Temporal and latitudinal variations of stratospheric trace gases: A critical comparison between theory and experiment, *J. Geophys. Res., 83*, 364-378, 1978.

Zuo, Y., and J. Hoigne, Evidence for photochemical formation of H_2O_2 and oxidation of SO_2 in authentic fogwater, *Science, 260*, 71-73, 1993.

D. J. Jacob and J. Liang, Division of Engineering and Applied Sciences and Department of Earth and Planetary Sciences, Harvard University, Pierce Hall, 29 Oxford St., Cambridge, MA 02138. (e-mail: djj@io.harvard.edu)